OPTICAL METABOLIC IMAGING OF TUMORS TO QUANITFY REACTIVE OXYGEN SPECIES

An Undergraduate Research Scholars Thesis

by

RANIYAH IMTIYAZ NATHANI

Submitted to the LAUNCH: Undergraduate Research office at
Texas A&M University
in partial fulfillment of requirements for the designation as an

UNDERGRADUATE RESEARCH SCHOLAR

Approved by
Faculty Research Advisor: Dr. Alexandra Walsh

May 2022

Major: Biomedical Engineering

RESEARCH COMPLIANCE CERTIFICATION

Research activities involving the use of human subjects, vertebrate animals, and/or biohazards must be reviewed and approved by the appropriate Texas A&M University regulatory research committee (i.e., IRB, IACUC, IBC) before the activity can commence. This requirement applies to activities conducted at Texas A&M and to activities conducted at non-Texas A&M facilities or institutions. In both cases, students are responsible for working with the relevant Texas A&M research compliance program to ensure and document that all Texas A&M compliance obligations are met before the study begins.

I, Raniyah Imtiyaz Nathani, certify that all research compliance requirements related to this Undergraduate Research Scholars thesis have been addressed with my Research Faculty Advisor prior to the collection of any data used in this final thesis submission.

This project required approval from the Texas A&M University Research Compliance & Biosafety office as displayed below.

TAMU IBC #: 2019-131 Approval Date: 10/21/2021 Expiration Date: 10/30/2022

TABLE OF CONTENTS PAGE

ABSTRACT 1

DEDICATION 3

ACKNOWLEDGEMENTS 4

NOMENCLATURE 6

1. INTRODUCTION 7

    1.1 Cancer and Tumor Heterogeneity 7
    1.2 Tumor Heterogeneity 7
    1.3 Cellular Metabolism: A Cause for Tumor Heterogeneity 8
    1.4 Reactive Oxygen Species (ROS) 10
    1.5 Reactive Oxygen Species and Optical Metabolic Imaging 12

2. METHODS 14

    2.1 Cyanide Experiment 14
    2.2 Optical Imaging Microscopy Experimental Setup 15
    2.3 Image Analysis 17

3. RESULTS 19

    3.1 Fluorescence Imaging Microscopy 19
    3.2 ROS Images 20
    3.3 Mean Intensity Redox Ratio 20
    3.4 ROS Prescence Before and After Cyanide 22

4. DISCUSSION 23

    4.1 Future Direction 24

5. CONCLUSION 26

REFERENCES 27

APPENDIX 30

ABSTRACT

Optical Metabolic Imaging of Tumors to Quantify Reactive Oxygen Species

Raniyah Imtiyaz Nathani
Department of Biomedical Engineering
Texas A&M University

Research Faculty Advisor: Dr. Alexandra Walsh
Department of Biomedical Engineering
Texas A&M University

The growth and development of cancer cells differs from that of normal cells. Cancer cells exhibit increased metabolic activity and have increased production of highly reactive molecules called Reactive Oxygen Species (ROS), which serve as regulators of important signaling pathways and promote many aspects of tumor growth and progression. Factors such as environmental changes, genetic mutations, and changes in the cellular and extracellular mechanical properties stimulate metabolic and functional heterogeneity to arise among tumor cells within the same patient. This has led to increased resistance to cancer treatments and greater difficulty in predicting how a patient's cancer will progress. To best address the relationship between cellular metabolism and tumor heterogeneity, optical imaging microscopy is employed to detect fluorescence signals of a ROS label and NADH, an important molecule in the process of cellular energy metabolism. A cyanide experiment is conducted to induce ROS in KRC cells, and ROS fluorescence assay is subsequently used to quantify ROS production. Fluorescence images of KRC cells before and after the cyanide experiment are acquired. Results demonstrate that both the optical redox ratio and ROS increased after the addition of cyanide compared to control cells without cyanide. While more

experimental trials need to be conducted, current experimental outcomes relay the potential for using the relationship between NADH redox state and ROS levels to look at different phases of the cell metabolic cycle to quantify tumor heterogeneity in the future. This can help extend our understanding of the parallel between tumor treatment response and metabolically distinct tumor cell populations which is currently not well understood.

DEDICATION

I would like to dedicate this body of work to those who are fighting cancer, and to past, current, and future scholars that are working hard in this field to help improve the diagnosis and treatment of cancer.

ACKNOWLEDGEMENTS

Contributors

I would like to thank my faculty advisor, Dr. Alexandra Walsh, for her constant guidance and support throughout my research project and my time in the lab.

I would also like to thank Linghao Hu and Anna Theodossiou, current PhD students in the Quantitative Optical Imaging Lab, who guided me through my microscopic imaging procedure. In addition, I would like to thank Uyen Nguyen, a current undergraduate student in the lab, for helping me learn the process of cell culturing.

Thanks also go to my friends and colleagues and the department faculty and staff for making my time at Texas A&M University an insightful and remarkable experience.

Finally, last but certainly not least, thanks go to my family for their encouragement and ceaseless support. This would not have been possible without their love and patience for believing in me.

The data used for Optical Metabolic Imaging of Tumors to Quantify Reactive Oxygen Species were generated by myself. The analysis depicted in Optical Metabolic Imaging of Tumors to Quantify Reactive Oxygen Species was conducted by myself with the help of my research advisor, Dr. Alexander Walsh.

Funding Sources

Undergraduate research was supported by the Biomedical Engineering Department at Texas A&M University.

This work was also made possible in part by Air Force Office of Scientific Research (AFOSR) under Grant Number FA9550-20-1-0078, Cancer Prevention and Research Institute of

Texas (CPRIT) under Grant Number RP200668, and the Texas A&M Engineering Experiment Station (TEES). Its contents are solely the responsibility of the authors and do not necessarily represent the official views of the AFOSR, CPRIT, nor the TEES.

NOMENCLATURE

ATP	Adenosine triphosphate
DNA	Deoxyribonucleic acid
ETC	Electron Transport Chain
FAD	Flavin adenine dinucleotide
$FADH_2$	Dihydroflavine-adenine dinucleotide
FLIM	Fluorescence-Lifetime Imaging Microscopy
ITH	Intratumor heterogeneity
NAD	Nicotinamide adenine dinucleotide
NADH	Reduced nicotinamide adenine dinucleotide
OMI	Optical Metabolic Imaging
PKC	Protein Kinase C
ROS	Reactive Oxygen Species

1. INTRODUCTION

1.1 Cancer and Tumor Heterogeneity

Two patients with the same cancer can respond differently to the same treatments [1]. Until recently, tumor cells were assumed to be identical to one another at any given stage of the cancer. However, researchers are observing that cells within the tumor can be extremely diverse. This means that when a biopsy is conducted, a fraction of the tumor cells that are collected may not be representative of the entire tumor causing important clinical features to be overlooked. Moreover, as cancer progresses, tumor heterogeneity increases leading to resistance to treatments. Unfortunately, this also results in greater difficulty for physicians and healthcare professionals to predict how a patient's cancer will progress and respond to treatments. This difference between cells within a tumor leverages the need to understand tumor heterogeneity in detail.

1.2 Tumor Heterogeneity

Variances among the tumor cells occur due to the presence of distinct molecular signatures that enable them to develop varying ranges of sensitivity to treatments. These heterogeneities can be classified into 3 categories: inter-tumor heterogeneity, inter-site heterogeneity, and intratumor heterogeneity (ITH) [2]. Inter-tumor heterogeneity, also denoted as inter-patient heterogeneity, describes tumor variation that occurs from patient to patient. This can occur due to the tumor microenvironment which may influence the increase or decrease in progression of cell mutation in patients. Inter-site heterogeneity relays the variation in tumor within an individual patient. As tumor cells begin to migrate or metastasize to different regions in the body, they may become aggressive and more difficult to treat depending on where they are. Lastly, ITH describes tumor variation in cellular population within a tumor. A small group of samples of these type of tumor

cells is regarded as tumor subclones which simply reflect their genetically diverse sub-population of cells [3]. Interestingly, ITH may explain why some cancer patients may go into relapse after responding successfully to treatment in the first round. The diversity present within the tumor subclones may allow a particular cell to continue to grow and reproduce and eventually transform into a drug-resistant tumor. In this way, tumors are very complex as they can contain different physical and genetic characteristics contributing to their variation even amongst each other. Factors such as the patient's genetics, environmental factors, and exposure shape the complexity of stages of tumor development and progression allowing this diverse disease to vary from person to person.

1.3 Cellular Metabolism: A Cause for Tumor Heterogeneity

The cellular metabolism process is quite complex as it comprises of controlled biological and chemical reactions that carry out essential processes such as synthesis and breakdown/removal of molecules. Within this process, two distinct molecules, NADH and $FADH_2$, play a key role in translating glucose into ATP or energy for the cell. An important redox carrier, both NAD+ and FAD+ molecules transform into NADH and $FADH_2$, respectively, and serve as acceptors of high energy electrons carrying them to the electron transport chain for the synthesis of ATP [4]. This is demonstrated in **Figure 1.1**.

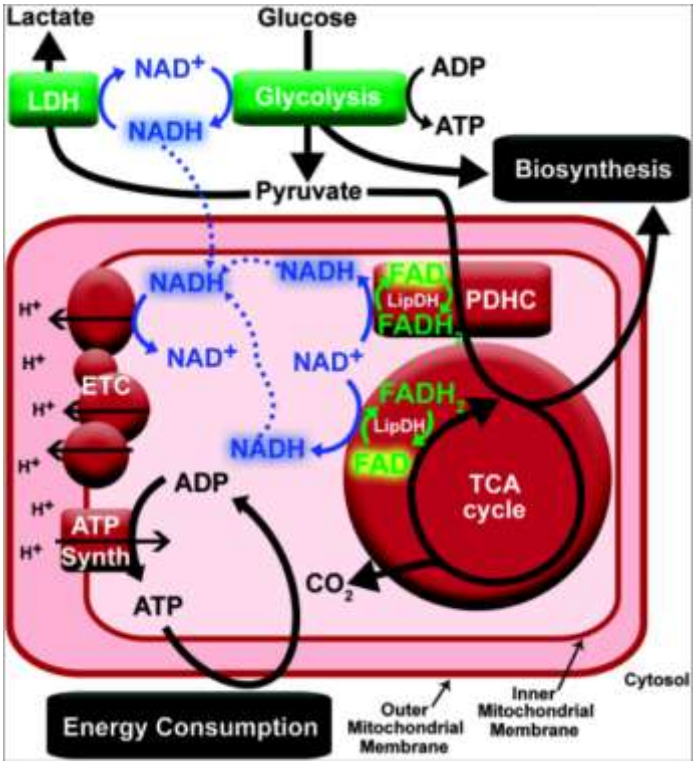

Figure 1.1: Roles of NADH and FAD in Cell Metabolism [5].

For a long time, it has been known that cellular metabolism of cancer cells is different from that of healthy cells. Cancer cells require increased energy compared to that of normal cells and therefore, have altered metabolic pathways that help to accommodate their accelerated growth, proliferation, metastasis, and adaptation. A study published in the Nature Reviews Clinical Oncology conducted an experiment where they studied cancer cells and chose to focus on glucose, glutamine, and lactate within the cells for their key role in the cellular metabolism process [6]. Using different techniques, they varied the levels of each of the molecules and observed their outcomes [6]. The results conveyed that when the glucose concentration and the lactate concentration increased, proliferation, acidity, and the Warburg effect increased [6]. The study also found that when glutamine increased glutamine addiction increased as well [6]. Essentially, the study pointed out that "[cancer] could harbor a small population of quiescent drug-tolerant

cells that have survived owing to adaptive activation of alternative metabolic pathways, surviving signals and epigenetic programs" [3, 6]. Importantly, other studies have relayed that shifts in these metabolic pathways promote mutations to arise [6, 7]. Therefore, studying metabolic pathways of cancer cells can provide crucial information about their functions which can be used to advance solutions to halt their biological processes.

Intriguingly, the roles of NADH and $FADH_2$ are not just limited to cellular energy production, but also in the growth and proliferation of the cell in response to a changing microenvironment [7]. During the developmental phase, cancer cells depict changes in oxygen levels wherein they express low oxygen levels [7]. This may stem from dysfunctions in the cell's mitochondria. Dr. Otto Warburg, a Nobel prize winner, hypothesized that "prime cause of cancer is the replacement of respiration of oxygen in normal body cells by fermentation of sugar [7]. In other words, he pointed out that cancer cells may reprogram their metabolism through which NADH and FAD cofactors help to promote changes in the metabolic fluxes of the cells [7]. In addition to cofactors, studies have also indicated strong interest in ROS or Reactive Oxygen Species for their role in metabolic dysfunction and signal transduction [8].

1.4 Reactive Oxygen Species (ROS)

Changes in cellular metabolism and high metabolic activity have resulted in an increase in ROS [8]. ROS are ions, molecules, or radicals with an unpaired electron in the outermost electron shell which makes them prone to 'steal' electrons from other molecules [9]. This makes ROS highly reactive which may be problematic to macromolecules such as DNA, lipids, and proteins [9]. For instance, in the presence of ROS, guanine in the DNA is modified causing it to pair with not only cytosine but also adenine [10]. This is one of many examples that showcase the occurrence of mutation within the cell. However, moderate levels of ROS are required for cellular functions.

In fact, a balanced ROS level is required to maintain redox homeostasis in the body which is necessary to ensure that appropriate signaling pathways are being cascaded. It is found that each cell is typically exposed to approximately 1.5 x 10^5 oxidative hits per day [11, 12]. At high levels of ROS, cells experience increased exposure to oxidative hits resulting in a condition known as oxidative stress which is commonly observed in cancer [11, 12]. Understanding this dual nature of ROS is critical to understanding its presence among tumor cells. While extremely high and low levels of ROS can induce physiological and biochemical damage to the cell, normal levels promote host defense against pathogenic microorganisms and help activate the immune system [11]. **Figure 1.2** illustrates the outcome of ROS imbalance by demonstrating how increased production of ROS due to a mutation induces production of protein kinase C (PKC) which further releases calcium contributing to cancer cell proliferation [12].

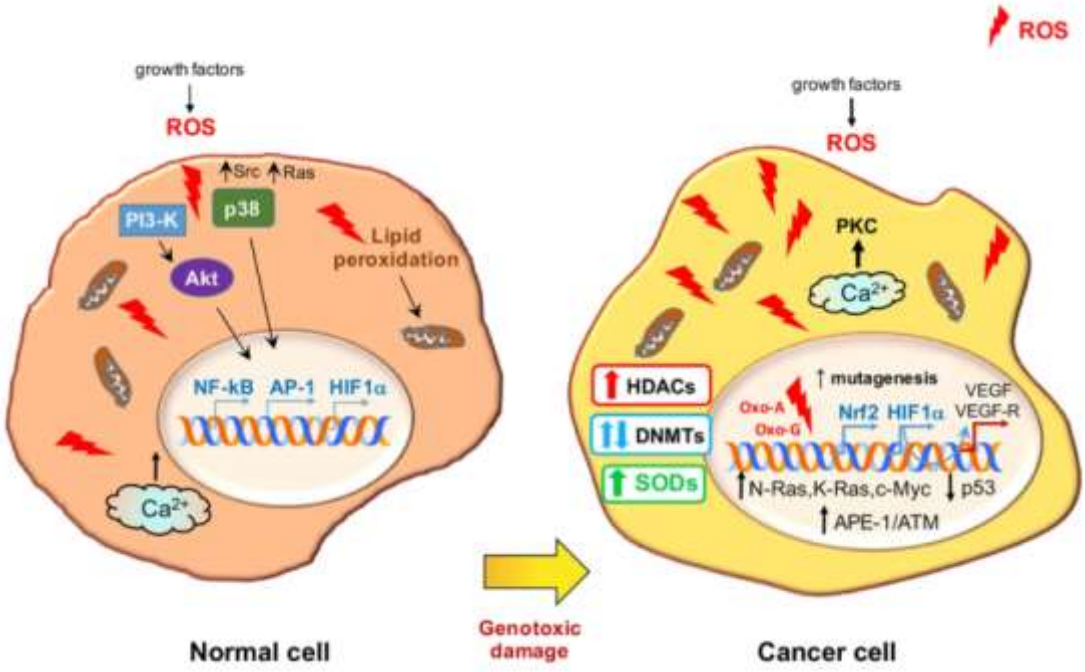

Figure 1.2: Changes to Within Signaling Cascade Following Mutation [12].

Another study also asserted that continuous activation of aerobic glycolysis can be correlated to oncogenes which can overall stimulate cancer progression [13, 14]. In this way, research has underscored the overlap between cellular metabolism and ROS. An important aspect to consider as well is that reduced forms of NADH and FAD have been known to protect against the toxicity of ROS. Thus, when NADH and FAD levels are affected or modified, cells develop greater risk for damage and begin to function abnormally due the potential damage from the presence of ROS. This attempts to provide a possible justification for an observation made by a study that stated that late-stage cancers produce their own antioxidants to fight toxic substances or ROS thus allowing them to further grow and proliferate [12]. Earlier stages do not seem to have this mechanism which explains why chemotherapy and radiation therapy may not work in late-stage cancers [12]. Developing clarity in the relationship between ROS and cellular metabolism can likely offer insight into the altered metabolism of cancer cells and mechanisms for their heterogeneity.

1.5 Reactive Oxygen Species and Optical Metabolic Imaging

Optical imaging is a valuable technique that provides nondestructive examination of dynamic changes in cellular and tissue processes both in vitro and in vivo. Through light-matter interaction, it can convey morphological and biochemical information of both cells and tissues. One of the many advantages of this method is its ability to detect intrinsic fluorophores of cells such as NADH and FAD which can be very useful to monitor cellular metabolism [5]. Through the selection of specific excitation and emission bands, optical imaging microscopy can isolate NADH and FAD fluorescence and provide optical contrast. The optical redox ratio is then calculated as the ratio between NADH and FAD to quantify cellular metabolism [5]. Moreover, assays can be performed on cells and tissues to identify ROS whose fluorescence can be detected and quantified by the imaging modality as well. Together, this can provide information regarding

tumor heterogeneity for possible signs of early cancer development in cells. Currently, optical imaging has been conducted on mesenchymal stem cells and in live kidney tissue and results have indicated that ROS can contribute to kidney disease and cancer [15]. In addition, optical imaging has also been applied to zebrafish xenograft tumors which have indicated that a variation of drug response was found in different resistant tumors [16].

Despite significant research indicating a direct correlation between cellular metabolism and tumor heterogeneity, the relationship between metabolic shifts and the development of distinct tumor cell populations is not well comprehended. Optical imaging micrscopy provides an opportunity to further explore this relationship in hopes of uncovering deterministic findings related to specific changes in ROS that induce changes in NADH and FAD levels. The purpose of this study is to perform both optical imaging and assays to assess the interconnection between cellular metabolism and ROS in cells. The NADH redox state and ROS levels can then be used to look more in-depth into the different phases of the cell metabolic cycles to quantify tumor heterogeneity.

2. METHODS

2.1 Cyanide Experiment

KRC cells were used to analyze the relationship between their ROS production and NADH redox ratio. The cells were cultured in 10 mL of media with 10% fetal bovine solution and 1% penicillin: streptomycin. Approximately 24 hours prior to imaging, cells were trypsinized with 2 mL of 0.25% of Trypsin solution for detachment, neutralized with 10 mL of media, collected via centrifugation in a 15 mL centrifuge tube, and resuspended in 1 mL of media. Next, 20 uL of cells/mL of media was placed on 35 mm glass bottom imaging dishes pre-filled with 2 mL of media. A total of 5 dishes were prepared: first dish served as the control group in which the metabolism of the cells was undisturbed, the second, third, and fourth dish served to analyze cells after disruption to their cellular processes, and the fifth dish served as an extra dish. This is relayed in **Figure 2.1.** The cells were incubated at 37 °C, 95% humidity, and 5% CO_2 overnight. Forty-five minutes prior to imaging, ROS-dye groups were incubated with 100 uL of 1000X ROS Deep Red Working Solution (Abcam, ab186029).

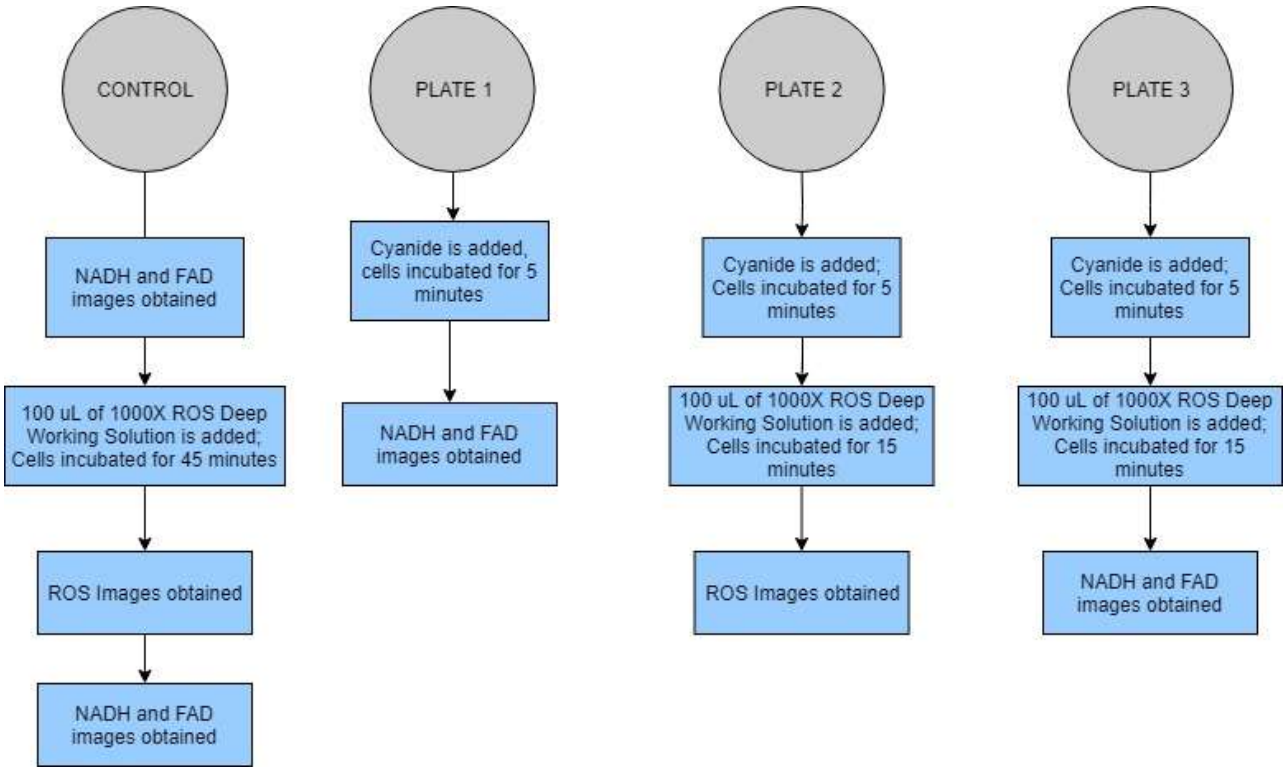

Figure 2.1: KRC-Cells Preparation.

A cyanide experiment was performed on KRC cells to induce ROS production [17]. Five-minutes prior to obtaining NADH and FAD images, 100 uL of 20X cyanide solution was added to Plate 1. In plate 2, 100 uL of 20X cyanide solution was added, cells were incubated for 5 minutes, 100 uL of 1000X ROS Deep Red Working Solution was added after which the cells were incubated for 15 more minutes before obtaining ROS images. In Plate 3, 100 uL of 20X cyanide solution was added, cells were incubated for 5 minutes, 100 uL of 1000X ROS Deep Red Working Solution was added after which the cells were incubated for 15 more minutes before obtaining NADH and FAD images.

2.2 Optical Imaging Microscopy Experimental Setup

The experimental setup consisted of 4 general components: Wide field fluorescence microscope, beam splitter, motorized micromanipulator, and the MicroManager software on the desktop. This setup is displayed in **Figure 2.2**.

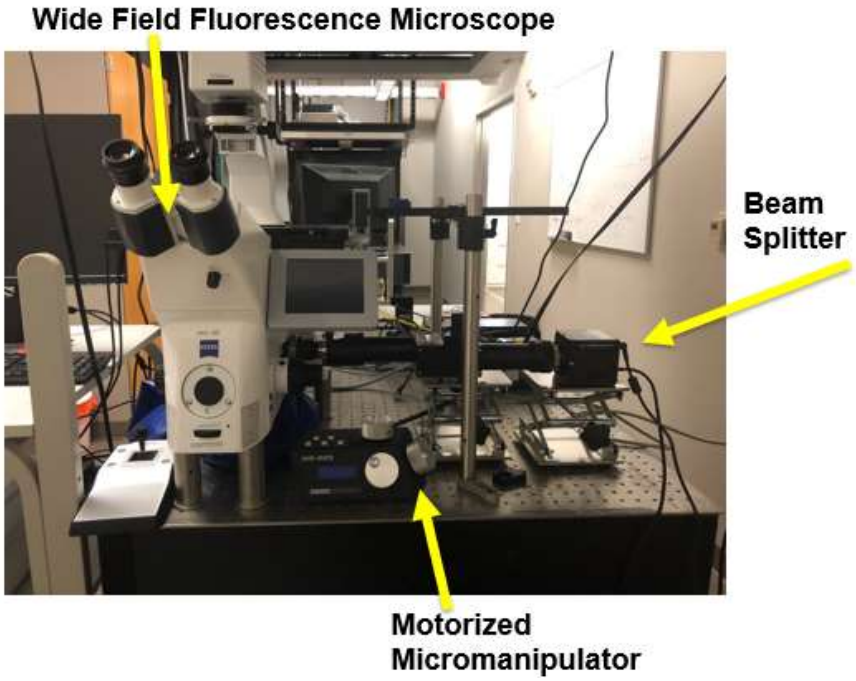

Figure 2.2: Experimental Setup.

Optical Imaging Microscopy was performed on a wide-field fluorescence microscope customized for NADH and FAD imaging within 4 hours to capture the changes in NADH redox ratio in correspondence to ROS production. Four trials were conducted. Optical imaging microscopy works by utilizing fluorescence intensities of NADH and FAD to monitor cellular metabolism. Because NADH and FAD have a distinct emission and absorption wavelength, when the molecules are excited, they emit autofluorescence. Interestingly, the beam splitter, as shown in **Figure 2.3,** allowed NADH and FAD images to be obtained simultaneously.

For NADH and FAD imaging, a white light source was filtered through a bandpass filter (313-400 nm) to excite NADH and FAD. The fluorescence emission was split using a dichroic mirror (496 nm) and NADH and FAD emission was re-aligned vertically and captured on a camera by a beam splitter. This beam splitter allowed us to image NADH and FAD simultaneously, rather than sequentially. For imaging ROS, a red filter was used. White light was filtered through a bandpass filter (625-650 ns) and fluorescence emission (650-700 nm) was captured by the camera.

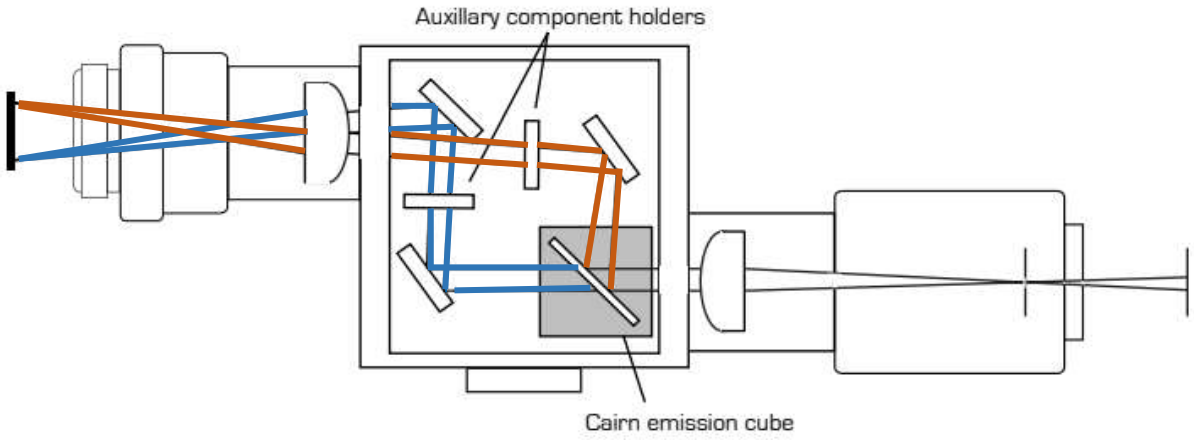

Figure 2.3: Beam Splitter [18].

2.3 Image Analysis

Optical Imaging Microscopy produced cell images were then analyzed in Cell Profiler. A pipeline in cell profiler was created which helped to determine the NADH and FAD levels, and then used these two known quantities to determine the NADH redox ratio. This pipeline consisted of multiple modules that cropped the image of interest using the 'Crop' module and then obtained the NADH and FAD measurement values using the 'ImageMath'. Subsequently, the 'MeasureImageIntensity' module was used to calculate the Redox Ratio.

Equation 1 displays the equation that was used within the 'MeasureImageIntensity' module to calculate the NADH intensity to FAD intensity to provide the Optical Redox Ratio (ORR) measurement.

$$ORR = \frac{NADH}{NADH + FAD} \quad \textbf{(1)}$$

The NADH redox ratios for each of the trials were then exported to a Microsoft Excel spreadsheet (.csv file). A python code was created to plot the data from the spreadsheet into a box and whisker plot for data analysis. Statistical analysis was conducted in Minitab. Lastly, images were processed for analysis via ImageJ software.

3. RESULTS

3.1 Fluorescence Imaging Microscopy

The wide-field fluorescence microscope was used to obtain autofluorescence images of the cells. **Figure 3.1** depicts these images.

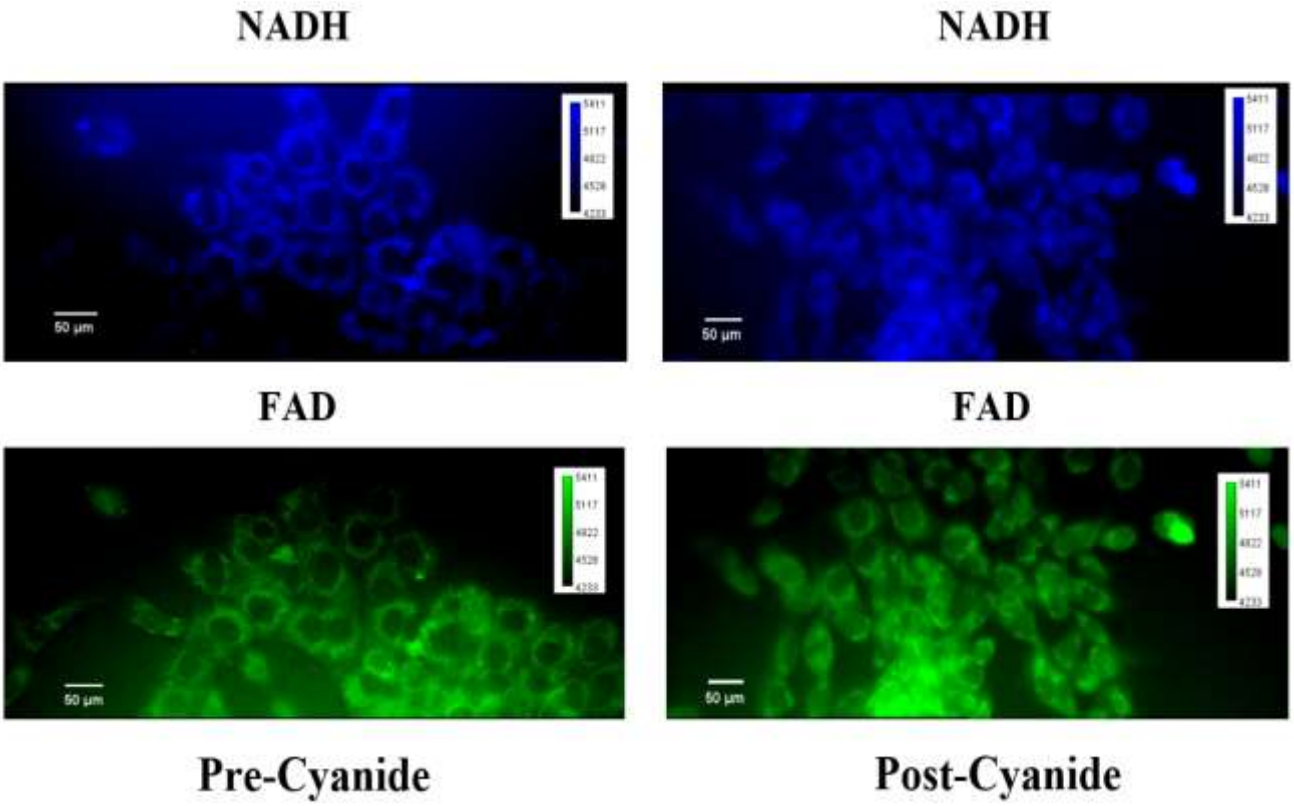

Figure 3.1: Sample of FLIM Images. Gray-scaled images are false-colored for improved visualization. NADH and FAD images before Cyanide [left] and NADH and FAD images after Cyanide [right] are displayed.

The images in **Figure 3.1,** depict clusters of cells grown in 2-D on the glass bottom dish. The nucleus is dark because NADH and FAD are primarily localized in the mitochondria and the cytosol of the cell. Simply looking at figures, it is observed that the NADH and FAD molecules appear brighter post-cyanide.

3.2 ROS Images

Upon directing a red-light wavelength of 650 nm at the cells, the microscope obtained the ROS images as shown in **Figure 3.2.** In contrast to the NADH and FAD images, ROS dye fluorescence brightness is correlated with ROS concentration. ROS is produced by the mitochondria which explains why they appear brighter than the rest of the cell.

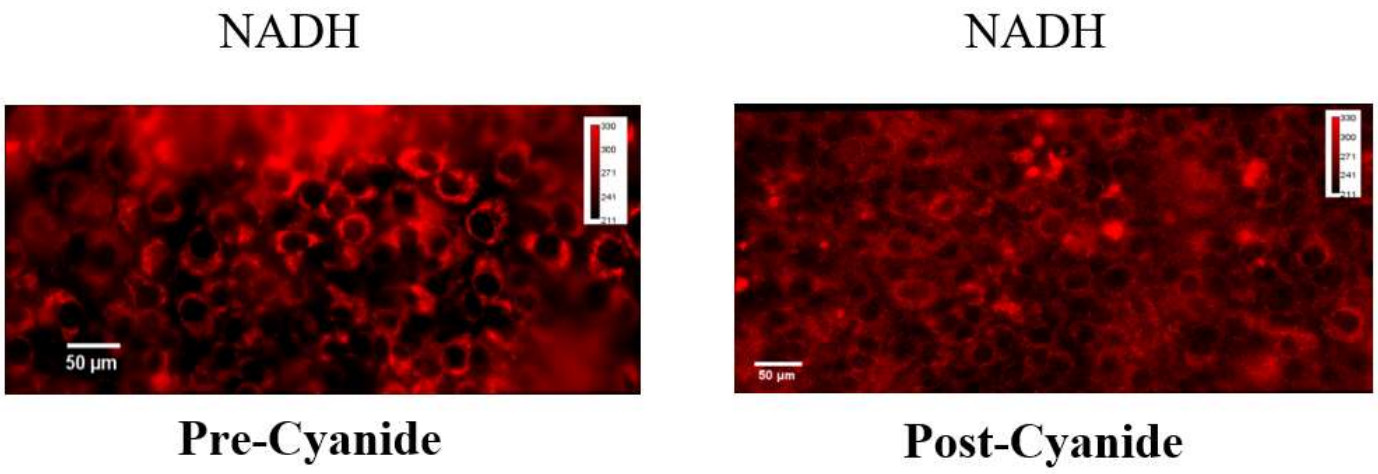

Figure 3.2: Sample of ROS Images Before Cyanide [left] and After Cyanide [right].

3.3 Mean Intensity Redox Ratio

After uploading all the images obtained into the CellProfiler pipeline, the Redox Ratio was then calculated and the resulting outcomes were exported in an Excel file as shown in **Table 3.1.** Analyzing the table, it can be observed that, overall, the mean intensity redox ratio seemed to increase after cyanide was added compared to before its addition.

Pre-Cyanide (no ROS)	Pre-Cyanide (with ROS)	Post-Cyanide (no ROS)	Post-Cyanide (with ROS)
0.561	0.549	0.569	0.563
0.548	0.525	0.576	0.548
0.487	0.523	0.549	0.542

Table 3.1: Mean Intensity Redox Ratio.

The box and whisker plots were then plotted using Python as seen in **Figure 3.3**. Four plots are depicted which represent the ORR of the KRC cells before the cyanide experiment with and without the ROS assay, and after the cyanide experiment with and without the ROS assay.

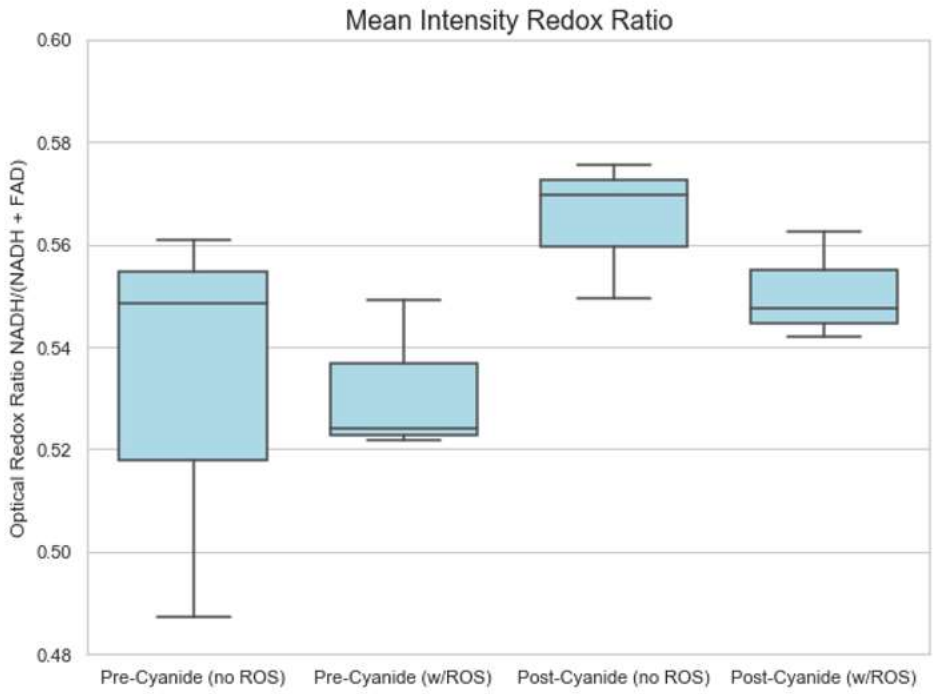

Figure 3.3: Mean intensity redox ratio for 4 fields of view from 3 independent experimental replicas. Statistical analysis ($p>0.05$).

3.4 ROS Prescence Before and After Cyanide

After uploading all the images obtained into the CellProfiler pipeline, the fluorescence intensity of the ROS dye was calculated, and the resulting outcomes were exported in an Excel file as shown in **Table 3.2**.

Pre-Cyanide	Post-Cyanide
0.115	0.160
0.035	0.070
0.034	0.050

Table 3.2: ROS Concentration before and after Cyanide.

The ROS production, alone, is also analyzed in the cells. Two plots are depicted which represent the ROS production of the KRC cells before the cyanide experiment and after the cyanide experiment as shown in **Figure 3.4**. A slight change in the ROS production was observed.

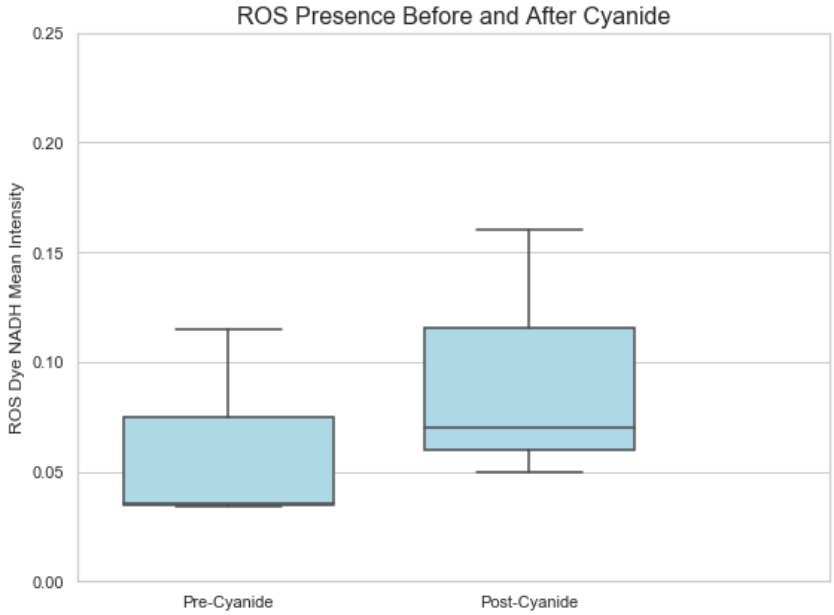

Figure 3.4: Fluorescence intensity of the ROS dye for 4 fields of view from 3 independent experimental replicas. Statistical analysis ($p>0.05$).

4. DISCUSSION

The goal of this research study was to explore the relationship between cellular metabolism and ROS production. While all cells have a basal level of ROS concentration that is needed to carry out their normal functions, extreme levels of ROS can disrupt cellular metabolic activity. Upon performing optical imaging microscopy, it was found that after cyanide was added to the cells, the intensities of NADH and FAD increased as reflected through the optical redox ratio. A comparison between pre-cyanide with and without ROS and its corresponding post-cyanide with and without ROS was conducted to simply observe whether the change in the optical redox ratio for NADH and FAD images acquired after addition of the ROS dye were comparable. The increase in the cofactors post-cyanide can be justified by the fact that cyanide is known to stop the cellular metabolism process by blocking the reduction of oxygen into water [19]. When this occurs, cells are deprived of oxygen and begin to experience hypoxia where production of folate mediated NADH continues, causing NADH to accumulate in toxic amounts [20]. Similar to the elevation of NADH and FAD, ROS concentration increased as was hypothesized. This observation is validated by the Journal of Basic and Applied Zoology which reported a study that relayed that cyanide is a neurotoxin that stimulates intracellular generation of ROS [21]. It relates that the bio-toxic effects could be mediated through the attack of generative reactive oxygen species on some target organs such as the liver, kidney, heart, and brain. Since the goal of the experiment is to understand the relation between ROS production with FAD and NADH quantities, the fact that cyanide stimulates increased generation of ROS can provide some insight into ROS and the cellular metabolism co-factors.

Interestingly, statistical analysis of both the optical redox ratio and ROS concentration concluded to be $p>0.05$. This relays that the null hypothesis, suggesting that the means of the different populations being analyzed are all equal, cannot be rejected. While a clear increase is seen in both the optical redox ratio and ROS concentration in **Figures 3.3 and 3.4**, the change is very small. This slight change may be due to multiple reasons including the possibility that not enough time was given for the cells to be exposed to the cyanide and the ROS dye before imaging. In this case, the cellular metabolism would not be properly disturbed causing a lower elevation of ROS than expected and even a smaller amount to be detected. For this reason, in the future, more time will be allotted for the cells to become used to the cyanide and the dye. Another possible source of error may originate from the images itself. Looking back at the ROS images in **Figure 3.2**, the light red spots near the cells in the corner of the images indicate background noise that may be coming from light nearby or shadow casted by a clump of cells. The wide-field fluorescence system is noisy due to the inclusion of scattered light and from out-of-plane fluorophores, such as clumping cells. The presence of noise justifies a probable cause for a smaller change in the ROS concentration before and after cyanide was added. It is proposed that a confocal microscopy or multiphoton microscope be used in the future to reduce the noise occurrence. Another source for the background noise may be attributed to the media in which the cells were placed in which may have reflected a lot of the light causing the images to not be as clear. Another change that can be implemented in future trials is the use of PBS solution instead of media to image the cells.

4.1 Future Direction

Despite the statistical analysis results, the data outcome conveyed that fluorescence imaging microscopy can be used to explore cellular metabolism of cells. Using autofluorescence

imaging is both valuable and unique due to its label-free nature and its ability to produce images that relay spatial context that is typically lost in traditional biochemical assays. As a future direction, this investigation will be expanded to observe cells in 3-D instead of 2-D using tumor and normal-derived organoids. Since in-vitro organoids consider the histopathological aspects of the tumor, and therefore, reveal insight into the intra-tumor heterogeneity of cancer cells, this investigation can provide significant information with regards to the association of tumor heterogeneity at different phases of the cell metabolic cycle. Likewise, changes the ROS production and ORR in the organoids at cell level will be quantified via optical imaging microscopy. This can help extend our understanding of the parallel between tumor treatment response and metabolically distinct tumor cell populations which is currently not well understood.

5. CONCLUSION

Many studies that have been conducted so far to understand cellular metabolism of cancer cells have employed biochemical mechanisms. Hence, this study attempted to approach this topic with a different perspective by deploying fluorescence imaging microscopy. The goal of this research study is to study the effects of ROS production on the cellular metabolism of the cells which is quantified through the calculation of the ORR measurement. Upon data analysis, it is seen that after the cyanide experiment, both the mean intensity redox ratio and the ROS production increased by a small amount. While the mean intensity experienced a greater change, the results, so far, demonstrate that both the optical redox ratio and ROS increased after the addition of cyanide compared to before its addition. However, more trials will be needed to confirm this. In summary, the outcomes give light to the fact that NADH levels may increase to regulate ROS concentrations and we can further use the data to investigate specific phases of the cellular metabolism cycle. Interestingly, this research can help to contribute towards ongoing cancer studies to better understand the cellular metabolism cycle within difference phases of cancer in patients.

REFERENCES

[1] N. C. Institute, "Cancer Statistics ". [Online]. Available: https://www.cancer.gov/aboutcancer/understanding/statistics.

[2] L. Zhu et al., "A narrative review of tumor heterogeneity and challenges to tumor drug therapy," (in eng), Ann Transl Med, vol. 9, no. 16, pp. 1351-1351, 2021, doi: 10.21037/atm-21-1948.

[3] H. F. Cabanos and A. N. Hata, "Emerging Insights into Targeted Therapy-Tolerant Persister Cells in Cancer," (in eng), Cancers (Basel), vol. 13, no. 11, p. 2666, 2021, doi: 10.3390/cancers13112666.

[4] Y. Htet and A. G. Tennyson, "NAD+ as a Hydride Donor and Reductant," Journal of the American Chemical Society, vol. 138, no. 49, pp. 15833-15836, 2016/12/14 2016, doi: 10.1021/jacs.6b10451.

[5] O. I. Kolenc and K. P. Quinn, "Evaluating Cell Metabolism Through Autofluorescence Imaging of NAD(P)H and FAD," (in eng), Antioxid Redox Signal, vol. 30, no. 6, pp. 875-889, Feb 20 2019, doi: 10.1089/ars.2017.7451.

[6] Nature Reviews Clinical Oncology, vol. 15, no. 2, pp. 81-94, 2018/02/01 2018, doi: 10.1038/nrclinonc.2017.166.

[7] N. Hammoudi, K. B. R. Ahmed, C. Garcia-Prieto, and P. Huang, "Metabolic alterations in cancer cells and therapeutic implications," (in eng), Chin J Cancer, vol. 30, no. 8, pp. 508-525, 2011, doi: 10.5732/cjc.011.10267.

[8] S. Romero-Garcia, J. S. Lopez-Gonzalez, J. L. Báez-Viveros, D. Aguilar-Cazares, and H. Prado-Garcia, "Tumor cell metabolism: an integral view," (in eng), Cancer Biol Ther, vol. 12, no. 11, pp. 939-948, 2011, doi: 10.4161/cbt.12.11.18140.

[9] "Mitochondria, Reactive Oxygen Species (ROS), and Their Effect on the Body," in *The Protein Man's Blog | A Discussion of Protein Research*, G-Biosciences, Ed., ed. G-Biosciences G-Biosciences 2021.

[10] H. J. Shields, A. Traa, and J. M. Van Raamsdonk, "Beneficial and Detrimental Effects of Reactive Oxygen Species on Lifespan: A Comprehensive Review of Comparative and Experimental Studies," (in English), *Frontiers in Cell and Developmental Biology*, Review vol. 9, 2021-February-11 2021, doi: 10.3389/fcell.2021.628157.

[11] S. J. Forrester, D. S. Kikuchi, M. S. Hernandes, Q. Xu, and K. K. Griendling, "Reactive Oxygen Species in Metabolic and Inflammatory Signaling," (in eng), *Circ Res*, vol. 122, no. 6, pp. 877-902, 2018, doi: 10.1161/CIRCRESAHA.117.311401.

[12] B. Perillo *et al.*, "ROS in cancer therapy: the bright side of the moon," *Experimental & Molecular Medicine*, vol. 52, no. 2, pp. 192-203, 2020/02/01 2020, doi: 10.1038/s12276-020-0384-2.

[13] X. Chang, X. Liu, H. Wang, X. Yang, and Y. Gu, "Glycolysis in the progression of pancreatic cancer," (in eng), *Am J Cancer Res*, vol. 12, no. 2, pp. 861-872, 2022. [Online]. Available: https://pubmed.ncbi.nlm.nih.gov/35261808

[14] M. Jang, S. S. Kim, and J. Lee, "Cancer cell metabolism: implications for therapeutic targets," Experimental & Molecular Medicine, vol. 45, no. 10, pp. e45-e45, 2013/10/01 2013, doi: 10.1038/emm.2013.85.

[15] A. Habibalahi et al., "Non-invasive real-time imaging of reactive oxygen species (ROS) using autofluorescence multispectral imaging technique: A novel tool for redox biology," (in eng), Redox Biol, vol. 34, pp. 101561-101561, 2020, doi: 10.1016/j.redox.2020.101561.

[16] N. Uyen et al., "Optical imaging of zebrafish xenograft tumors for a high throughput drugs screen," in Proc.SPIE, 2021, vol. 11622. [Online]. Available: https://doi.org/10.1117/12.2577637. [Online]. Available: https://doi.org/10.1117/12.2577637.

[17] H. E. Kadiri and S. O. Asagba, "The chronic effects of cyanide on oxidative stress indices in the domestic chicken (Gallus domesticus L.)," The Journal of Basic and Applied Zoology, vol. 80, no. 1, p. 30, 2019/05/03 2019, doi: 10.1186/s41936-019-0098-y.

[18] T. Photometrics. "OptoSplit II." https://www.photometrics.com/products/imaging-splitters/optosplit-ii.

[19] J. Hariharakrishnan, R. M. Satpute, G. B. Prasad, and R. Bhattacharya, "Oxidative stress mediated cytotoxicity of cyanide in LLC-MK2 cells and its attenuation by alpha-ketoglutarate and N-acetyl cysteine," (in eng), *Toxicol Lett,* vol. 185, no. 2, pp. 132-41, Mar 10 2009, doi: 10.1016/j.toxlet.2008.12.011.

[20] L. Yang *et al.*, "Serine Catabolism Feeds NADH when Respiration Is Impaired," *Cell Metabolism,* vol. 31, no. 4, pp. 809-821.e6, 2020/04/07/ 2020, doi: https://doi.org/10.1016/j.cmet.2020.02.017.

[21] H. E. Kadiri and S. O. Asagba, "The chronic effects of cyanide on oxidative stress indices in the domestic chicken (Gallus domesticus L.)," *The Journal of Basic and Applied Zoology,* vol. 80, no. 1, p. 30, 2019/05/03 2019, doi: 10.1186/s41936-019-0098-y.

APPENDIX

Pre-Cyanide	Post-Cyanide
0.125	0.203125
0.109375	0.125
0.109375	0.171875
	0.140625

Table A.1: Trial 1 ROS Concentration before and after Cyanide.

Pre-Cyanide (no ROS)	Pre-Cyanide (with ROS)	Post-Cyanide (no ROS)	Post-Cyanide (with ROS)
0.537062	0.53788	0.561180161	0.537308
0.552897	0.540042	0.55525022	0.577103
0.584742	0.559456	0.592065299	0.56631
0.569155	0.558873	0.601580433	0.569114

Table A.2: Trial 1 Mean Intensity Redox Ratio.

Pre-Cyanide	Post-Cyanide
0.046875	0.09375
0.015625	0.03125
0.046875	0.0625
0.03125	0.09375

Table A.3: Trial 2 ROS Concentration before and after Cyanide.

Pre-Cyanide (no ROS)	Pre-Cyanide (with ROS)	Post-Cyanide (no ROS)	Post-Cyanide (with ROS)
0.531912	0.555502	0.569828	0.513575
0.556397	0.529118	0.546392	0.563042
0.54973	0.523146	0.565269	0.528596
0.544791	0.513142	0.555965	0.583886
0.554192	0.518002	0.609941	0.544678
0.55322	0.506008	0.605752	0.550999

Table A.4: Trial 2 Mean Intensity Redox Ratio.

Pre-Cyanide	Post-Cyanide
0.03125	0.046875
0.03125	0.03125
0.046875	0.03125
0.03125	0.046875
0.03125	0.0625
0.03125	0.078125

Table A.5: Trial 3 ROS Concentration before and after Cyanide.

Pre-Cyanide (no ROS)	Pre-Cyanide (with ROS)	Post-Cyanide (no ROS)	Post-Cyanide (with ROS)
0.475105629	0.529918	0.556253	0.540702
0.476265406	0.531815	0.588777	0.535355
0.497191706	0.532161	0.538605	0.545262
0.497496223	0.509656	0.537506	0.535487
0.490635625	0.512286	0.5313	0.548591
0.486979894	0.513853	0.543356	0.546467

Table A.6: Trial 3 Mean Intensity Redox Ratio.